Coordinated Regulation of Pathways for Enhanced Cell Motility and Chemotaxis Is Conserved in Rat and Mouse Mammary Tumors

Weigang Wang,[1] Jeffrey B. Wyckoff,[1] Sumanta Goswami,[1,3] Yarong Wang,[1] Mazen Sidani,[1] Jeffrey E. Segall,[1] and John S. Condeelis[1,2]

[1]Department of Anatomy and Structural Biology and [2]Gruss Lipper Center for Biophotonics, Albert Einstein College of Medicine, Bronx, New York and [3]Department of Biology, Yeshiva University, New York, New York

Abstract

Correlating tumor cell behavior *in vivo* with patterns of gene expression has led to new insights into the microenvironment of tumor cells in the primary tumor. Until now, these studies have been done with cell line–derived tumors. In the current study, we have analyzed, in polyoma middle T oncogene (PyMT)–derived mammary tumors, tumor cell behavior and gene expression patterns of the invasive subpopulation of tumor cells by multiphoton-based intravital imaging and microarray-based expression profiling, respectively. Our results indicate that the patterns of cell behavior that contribute to invasion and metastasis in the PyMT tumor are similar to those seen previously in rat MTLn3 cell line–derived mammary tumors. The invasive tumor cells collected from PyMT mouse mammary tumors, like their counterparts from rat xenograft mammary tumors, are a population that is relatively nondividing and nonapoptotic but chemotherapy resistant and chemotactic. Changes in the expression of genes that occur uniquely in the invasive subpopulation of tumor cells in the PyMT mammary tumors that fall on the Arp2/3 complex, capping protein and cofilin pathways show a pattern like that seen previously in invasive tumor cells from the MTLn3 cell line–derived tumors. These changes predict an enhanced activity of the cofilin pathway, and this was confirmed in isolated invasive PyMT tumor cells. We conclude that changes in gene expression and their related changes in cell behavior, which were identified in the invasive tumor cells of cell line–derived tumors, are conserved in the invasive tumor cells of PyMT-derived mouse mammary tumors, although these tumor types have different genetic origins. [Cancer Res 2007;67(8):3505–11]

Introduction

Critical to an understanding of the process of cancer metastasis is the examination of the behavior of tumor cells that are metastasizing from the primary tumor. Correlating cell behavior *in vivo* with patterns of gene expression can lead to new insights into the microenvironment of carcinoma cells in the primary tumor and the molecular mechanisms behind cell behavior. We have used the xenograft model of the paired rat mammary cancer MTLn3/MTC cells to study the behavior of tumor cells during invasion and metastasis (1). Using multiphoton microscopy, we found five major differences in tumor cell behavior between the nonmetastatic MTC and metastatic MTLn3 cell line–derived primary mammary tumors involving differences in adhesion to extracellular matrix, cell motility, and chemotaxis. These behavioral differences were correlated with seven categories of molecules that were differentially expressed and related to these behaviors (1).

A xenograft tumor model was used in the above studies where a bolus of cells was injected into the mammary gland of the rat. Because these tumors do not show the usual histology and progression seen clinically, another animal model that is clinically relevant was chosen for further work on tumor cell behavior and expression profiling *in vivo*. Here, we used a mouse model of breast cancer that resembles the human disease in both morphology and progression, the polyoma middle T oncogene (PyMT)–derived mammary tumor (2, 3). Female mice carrying Cre recombinase driven by the mouse mammary tumor virus (MMTV) promoter, and *Cre*-activatable *EGFP* (*CAG-CAT-EGFP*; ref. 4) transgenes showed brightly fluorescent cells in the mammary gland and/or PyMT tumor (5). The ability to image tumor cells in transgenic animals allows, for the first time, the evaluation of tumor cell behavior in tumors that have developed directly from the mammary epithelium.

In the current study, using PyMT-derived mammary tumors, tumor cell behavior and gene expression patterns of the invasive carcinoma cells were analyzed by intravital imaging and microarray-based profiling, respectively. Our results show a different pattern of gene expression between the invasive tumor cells and the general population of tumor cells in the PyMT primary tumors. These differences can be related to the ability of the tumor cells to invade through the surrounding stroma and migrate into the blood vessels. We also show that changes in cell behavior and gene expression in the invasive tumor cells that were identified in the MTLn3 rat model, such as the activity status of the cofilin pathway and the proliferation and apoptosis status, are conserved in the invasive tumor cells of PyMT-derived mouse mammary tumors.

Materials and Methods

Mice. Transgenic mice were maintained on a segregating FVB-C3H/B6 background. The details of the origin and identification of *MMTV-PyMT, MMTV-Cre, CAG-CAT-EGFP*, and *MMTV-Cre/CAG-CAT-EGFP/MMTV-PyMT* mice have been described previously (4, 5).

Multiphoton microscopy. Tumor imaging using multiphoton microscopy was done as described previously (5). The objective used was a 20× Plan Apo 0.7 numerical aperture (air), and images were collected at a field size of 512 × 512 μm at a depth of 3–10 cell diameters into the tumor. Images were processed using NIH Image 1.61/ppc and Adobe Photoshop. Pixel intensity of fluorescence and second harmonic–generated photons was quantified by subtracting the background from the total pixel intensity of the region of interest.

Note: Supplementary data for this article are available at Cancer Research Online (http://cancerres.aacrjournals.org/).

Requests for reprints: John Condeelis, Department of Anatomy and Structural Biology, Albert Einstein College of Medicine, Bronx, NY 10461. Phone: 718-430-3547; Fax: 718-430-8806; E-mail: condeeli@aecom.yu.edu.

doi:10.1158/0008-5472.CAN-06-3714

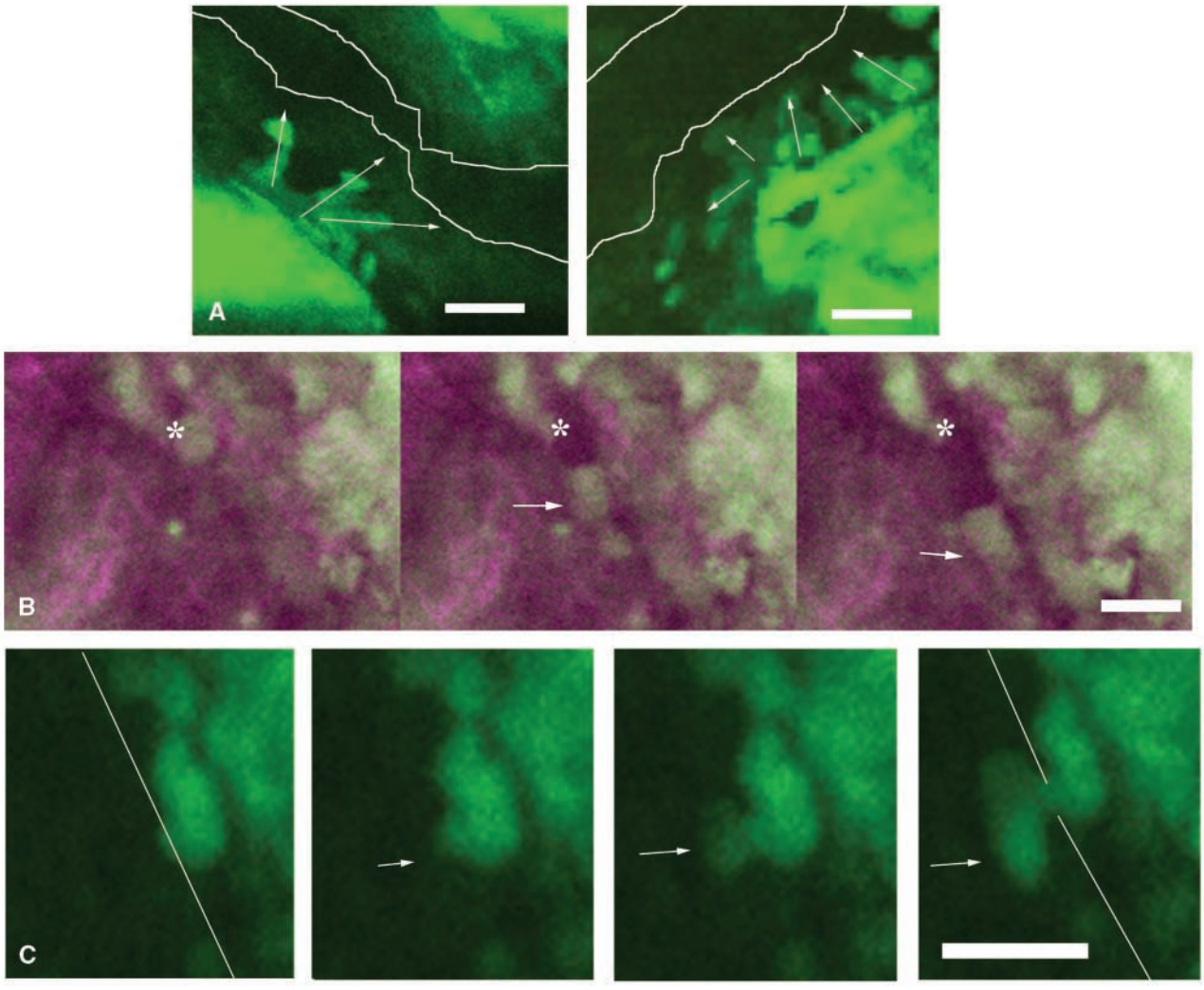

D

		ECM fiber-dependent	ECM fiber-independent
Host Cell Movement	Numbers of events / field	0.35	0.55
	Type of cell movement	39%	61%
Cancer Cell Movement	Numbers of events / field	1.25	0.8
	Type of cell movement	61%	39%

Figure 1. Multiphoton microscopy of tumor cells in a PyMT mammary tumor. *A,* GFP-labeled tumor cells (*green*) are frequently oriented toward blood vessels. Each panel shows an image of a blood vessel and surrounding tissue in two different PyMT tumors. In both panels, the white lines delineate the boundaries of blood vessels. Vectors indicate the long axes of individual tumor cells and indicate their polarity toward blood vessels. *B,* GFP-labeled tumor cell (*green*) is seen crawling along the collagen matrix (*purple*). Collagen is imaged by the creation of second harmonic–generated polarized light. *Arrows*, cell at different stages of movement. *, starting position of the cell. Frames are every 4 min. *C,* GFP-labeled tumor cell (*green*) is seen intravasating into a blood vessel. Line delineates vessel periphery. Arrows point to cell entering vessel. Frames are every 4 min. *Bar,* 25 μm. *D,* analysis of cell movements inside GFP PyMT primary tumors. Anesthetized animals were imaged using multiphoton microscopy, and time-lapse *z*-series movies were generated and analyzed. Cancer and host cell movements were further subdivided into ECM-dependent and ECM-independent translocation (see Materials and Methods). A total of 11 animals were imaged, and 20 movies were generated and analyzed.

Cell behavior analysis. Cancer cells were identified by their green fluorescent protein (GFP) fluorescence, whereas host cells were identified as shadows due to their ability to scatter light from the green tumor cells (5). Cancer and host cell movements were further subdivided in relation to their movement relative to extracellular matrix (ECM) fibers. ECM fibers were visualized by second-harmonic generation of scattered photons. Cell movements on ECM fibers were scored as (*a*) ECM-associated translocation and (*b*) cell movements not associated with ECM fibers. Each type of cell movement was recorded from 20 fields in 11 animals. Cell motility was visualized by time-lapse multiphoton microscopy by taking an image at 1-min intervals for at least 30 min. Motion analysis was carried out using two-dimensional Dynamic Image Analysis System software. The polarization

of tumor cells toward blood vessels was scored as described previously (6) as the percentage of blood vessels per 200 × 200 μm imaging field with four or more tumor cells adjacent to the vessel, with their long axes polarized toward the vessel. To account for tissue orientation that was not related to polarization of individual tumor cells toward vessels, tumor cells adjacent to a vessel were scored as randomly oriented with regard to vessels if neighboring cells more than two cell diameters distant from the vessel were also oriented toward the vessel.

Collection of invasive tumor cells and the general population of primary tumor cells. The invasive cells were collected from PyMT tumors using chemotaxis, with microneedles containing either epidermal growth factor (EGF) or colony-stimulating factor 1 (CSF1). Macrophages were removed from this population using MACS CD11b Microbeads (Miltenyi Biotec, Auburn, CA) as described previously (7). To isolate the general population of primary tumor cells, fluorescence-activated cell sorting (FACS) was done based on the GFP expression in tumor cells (7). In addition, a portion of the FACS-sorted tumor cells was also plated onto Matrigel and stimulated with EGF for 4 h. This is used to identify genes that are affected by FACS, Matrigel, and EGF-mediated collection. Changes in expression due to these stimuli were subtracted so that only changes in gene expression from the tumor microenvironment were scored (7).

Cell proliferation and apoptosis assays. The invasive and general population of primary tumor cells were allowed to adhere overnight in collagen-coated Mytek dishes in DMEM with 20% fetal bovine serum and gentamycin (50 μg/mL). Subsequently, bromodeoxyuridine (BrdUrd; BD Biosciences) was added to the cells in culture (10 μmol/L final concentration) and incubated overnight. Incorporation of BrdUrd in the cells was detected using BrdUrd *In situ* Detection Kit (BD Biosciences) following the manufacturer's protocol. The carcinoma cells were identified by the presence of GFP, and the proliferating cells were identified by the incorporation of BrdUrd in the nuclei. The nuclei were counterstained with 4′,6-diamidino-2-phenylindole for better identification. The results are presented as percentage of proliferating cells compared with all the carcinoma cells.

For apoptosis assays, the invasive tumor cells and general population of primary tumor cells were cultured and tested as described previously (8). The cells were challenged with tamoxifen (Sigma, St. Louis, MO; 5 μmol/L).

Barbed end assay. Quantification of free barbed ends in the invasive and general population of primary tumor cells was done as previously described (9).

RNA extraction, amplification, probe labeling, and microarray hybridization. RNA extraction, reverse transcription, SMART PCR amplification, microarray probe labeling, hybridization, and image collection were described in previous studies (7). Three independently isolated RNA samples were amplified and used to generate probes for the microarray analysis.

Quality control and significance analysis of microarrays. The scanned images were analyzed using the software Genepix (Axon Instruments, Foster City, CA), and an absolute intensity value was obtained for both the channels. The data filtering, global LOWESS normalization normalization, and significance analysis of microarrays (SAM) were done as described previously (7, 8). The SAM algorithm performs a significance analysis by comparing the relative variance of the replicates between the samples.

Real-time PCR confirmation. To verify the data obtained from microarrays, quantitative real-time PCR analysis of selected overexpressed and underexpressed genes was done using the ABI 7900 (Applied Biosystems, Foster City, CA) with sequence-specific primer pairs for all genes tested (see Supplementary Table S1 for primer sequences, amplicon size, and annealing temperature) as described previously (7, 8). Three independently amplified RNA samples were used for the real-time PCR assays, and each sample was tested in three independent repeats for all the genes analyzed. Housekeeping gene β-actin was used for normalization.

Results and Discussion

Patterns of cell behaviors that contribute to invasion and metastasis in the PyMT tumor. In our previous studies with cell line–derived tumors, tumor cell behaviors were observed in orthotopic models *in vivo* that relate to metastatic potential (1, 5, 6), such as (*a*) linear high-velocity motility of tumor cells along collagen fibers, (*b*) increased tumor cell polarity and locomotion toward blood vessels, and (*c*) the ability of metastatic tumor cells to

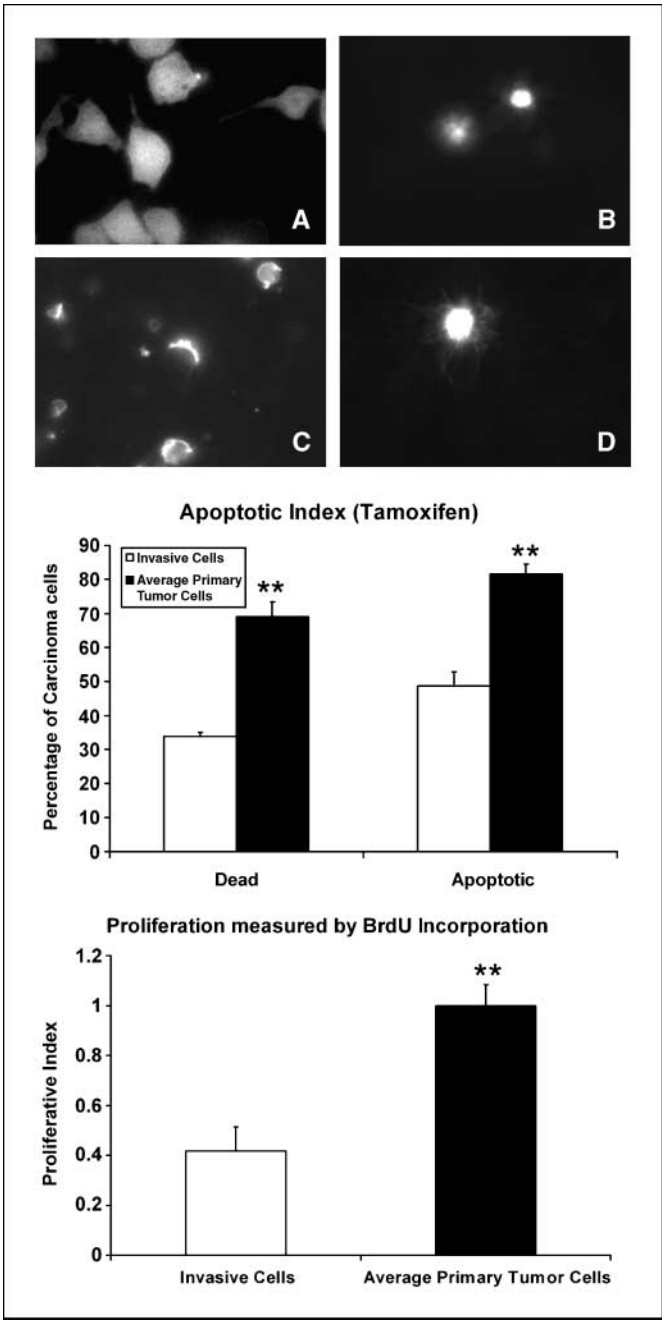

Figure 2. Invasive carcinoma cells show reduced apoptosis and proliferation compared with the general population of tumor cells and are resistant to tamoxifen. The general population of tumor cells collected by FACS sorting (average primary tumor cells) and invasive tumor cells collected by the *in vivo* invasion assay were tested for proliferation and apoptosis. Cells were treated with BrdUrd for 16 h, and the incorporation was detected using anti-BrdUrd antibody. Carcinoma (GFP-positive) cells (*A*), which were also BrdUrd positive (*B*), were counted in both the populations. *Bars,* SE of three separate experiments. For the apoptosis study, the annexin V–positive population (*C*) is considered apoptotic, whereas the propidium iodide–positive population (*D*) is considered as dead cells. The panels indicate separate fields. Apoptotic index was calculated by comparing the invasive and general population of primary tumor cells responding to tamoxifen challenge. **, $P < 0.01$.

Table 1. Differentially expressed genes in the minimum motility pathways are compared in the invasive tumor cells from both MTLn3 and PyMT mammary tumors

Genes support the minimum motility pathway	MTLn3 invasive cells	PyMT invasive cells
EGFR	2–20	NC
PI3 kinase δ 110	NC	3
PLC δ	NC	2
RhoA	2	NC
CDC42	4	12
ROCK1	2–3	NC
PAK1	NC	3
PKCz	3	NC
PIP5K	3	3
Capping protein	2–5	2
MENA	4	3
EVL	NC	4
LIMK1	3	2
SSH1	NC	3
Cofilin 1	2	NC
Arp2/3	2-6	4–5
ZBP1	0.1–0.25	0.4
WAVE3	2	NC

Abbreviation: NC, no change.

remain intact during intravasation. In the current study, several behaviors seen previously in cell line–derived tumors were observed again in the PyMT tumors. As shown in Fig. 1, these common behaviors are as follows:

- Tumor cells in primary PyMT mammary tumors move as solitary cells at up to 10 times the velocity seen *in vitro*. The highest velocities (3.9 ± 0.28 μm/min) are observed for tumor cells in PyMT tumors that are moving along linear paths in association with ECM fibers.
- Tumor cells in PyMT tumors are polarized toward blood vessels. Tumor cell polarization toward blood vessels was scored blind as described previously (6). We found that 68 ± 4.5% of vessels in PyMT mammary tumors at 16 to 18 weeks had tumor cells polarized toward them (n = 113 vessels in 30 fields, SE) consistent with what was seen in cell line–derived metastatic mammary tumors studied previously (6, 10). Furthermore, tumor cell movement has been shown to occur most frequently around blood vessels and the invasive front of the tumor in association with macrophages in PyMT mammary tumors (11).
- As shown in Fig. 1 and Supplementary Movies S1 to S3, host and tumor cell migration was scored in relation to their movements on ECM fibers and in relation to each other. Our results show that both host and tumor cells exhibit ECM fiber-dependent and fiber-independent migration, whereas the tumor cells had both a higher frequency of movement and ECM fiber-dependent movement, compared with the host cells.

The invasive cells are less proliferating and more apoptotic. Ideally, to understand motility, invasion, and metastasis, the invasive tumor cell population must be isolated and directly studied. Based on the chemotaxis of tumor cells to blood vessels, we have developed an *in vivo* invasion assay, which allows us to collect invasive cells from live primary tumors in mice and rats using chemotaxis to microneedles containing chemoattractants like EGF and CSF1 to mimic chemotactic signals from blood vessels and surrounding tissue (5, 11). Using this method to collect invasive tumor cells from MTLn3 cell-derived primary tumors, we have shown in our previous studies that the invasive tumor cells are a population that is neither dividing nor apoptotic (7, 8).

In the current study, we tested the apoptosis and proliferation status in the invasive tumor cells collected from the PyMT-derived mammary tumors of transgenic mice using chemotaxis to determine if they resemble the properties of invasive tumor cells isolated from cell line–derived tumors. As shown in Fig. 2, the invasive tumor cells from PyMT tumors are both hypoapoptotic and hypoproliferative. The isolated invasive tumor cells show significantly reduced apoptosis and proliferation as compared with the general population of tumor cells that were FACS sorted from the primary tumor. These data also indicate that the invasive cells are resistant to chemotherapeutic drugs like tamoxifen. Therefore, the invasive tumor cells collected from PyMT mouse mammary tumors, like their counterparts from rat xenograft mammary tumors, are a population that is relatively nondividing and nonapoptotic but chemotherapy resistant.

The invasive tumor cells from MTLn3-derived and PyMT primary tumors share a similar invasion signature. The *in vivo* invasion assay has been used with array-based gene expression analysis to investigate the gene expression patterns of invasive tumor cells isolated from primary tumors by chemotaxis (7). By comparing gene expression patterns of invasive tumor cells collected using the *in vivo* invasion assay to those of the general population of tumor cells isolated from the same cell line–derived primary tumor, patterns of gene expression unique to the invasive subpopulation of cells were identified and characterize the invasive cells as being highly chemotactic (7, 8).

In the current study, microarray analysis was done on both the invasive and general populations of tumor cells collected from PyMT tumors, using the same strategy as in our previous studies (7, 8), to determine if a similar pattern of gene expression unique to invasive tumor cells was occurring in both cell line–derived and PyMT tumors. Differential gene expression analysis comparing the invasive and general population of PyMT primary tumor cells was done using SAM at 3% false discovery rate level. After removal of EGF and Matrigel-regulated genes along with expressed sequence tags with no homology to known genes, comparison of the invasive tumor cell subpopulation collected with the *in vivo* invasion assay with the general tumor cell population resulted in a set of about 900 genes in which expression is changed in the PyMT invasive tumor cell subpopulation (Supplementary Table S2). This gene list provides a general resource of possible targets for future anti-invasion therapy. For this report, we have analyzed this list from the perspective of cell motility and chemotaxis, which is critical to invasion during metastasis (12).

We have shown in a previous study using MTLn3 cell line–derived mammary tumors that the genes coding for the pathways leading to the three end-stage effectors (Arp2/3 complex, capping protein, and cofilin) of the minimum motility machine that regulates β-actin polymerization at the leading edge and, therefore, the motility and chemotaxis of carcinoma cells (9, 13, 14), were up-regulated in the invasive tumor cells from cell line–derived

mammary tumors (7). As shown in Fig. 3 and Table 1, the genes that are regulated in the invasive tumor cells from PyMT tumors that fall on the Arp2/3 complex, capping protein, and cofilin pathways show a similar pattern to that seen previously in invasive tumor cells from the MTLn3 cell line–derived tumors. Furthermore, the expression pattern derived for invasive cells from PyMT tumors was identical regardless of whether EGF or CSF1 was used to collect the invasive population of tumor cells (Fig. 3*B*). This result indicates that the paracrine-mediated relay chemotaxis between macrophages and tumor cells identified previously (5, 15) is involved in the collection of invasive tumor cells from PyMT tumors using the *in vivo* invasion assay. Furthermore, this result indicates that the microenvironment of the tumor, and not the collecting ligand, determines the gene expression profile of the invasive tumor cell population.

The Arp 2/3 complex, capping protein, and cofilin pathways interact to determine the motility and chemotaxis phenotype. Capping protein binds to the growing barbed ends of actin filaments to prevent further elongation. In invasive tumor cells, the patterns of regulation of genes of the capping protein pathway exhibit an antagonistic relationship similar to that seen in the cofilin pathway, where expression of both stimulatory and inhibitory branches are up-regulated together. The expression of the capping protein is increased by 2-fold. In addition, genes that antagonize capping protein function such as phosphoinositide-3-kinase δ 110, Cdc42, the type II α isoform of PIP5K and MENA/EVL (16) are up-regulated.

Both the cofilin and capping protein pathways converge on the Arp2/3 complex. Because the expression of key components of both pathways are up-regulated, it is interesting that the expression of several subunits of the Arp2/3 complex (the p16 and p21 subunits) are also greatly up-regulated in invasive cells, as is the expression of the upstream stimulator of the Arp2/3 complex, Cdc42. Cdc42 regulates neural Wiskott-Aldrich syndrome protein (N-WASP), which induces actin polymerization by activating Arp2/3 complex (17). Elevated expression of Cdc42, as observed in invasive cells, in combination with the elevated expression of Arp2/3 complex (Fig. 3*A*), will lead to increased invadopod production and cell invasion (18, 19). Cofilin and Arp2/3 complex synergistically contribute to the nucleation of a dendritic array both *in vitro* (20) and *in vivo* (21). This synergy results from the amplification of the Arp2/3 complex's nucleation activity by cofilin's severing

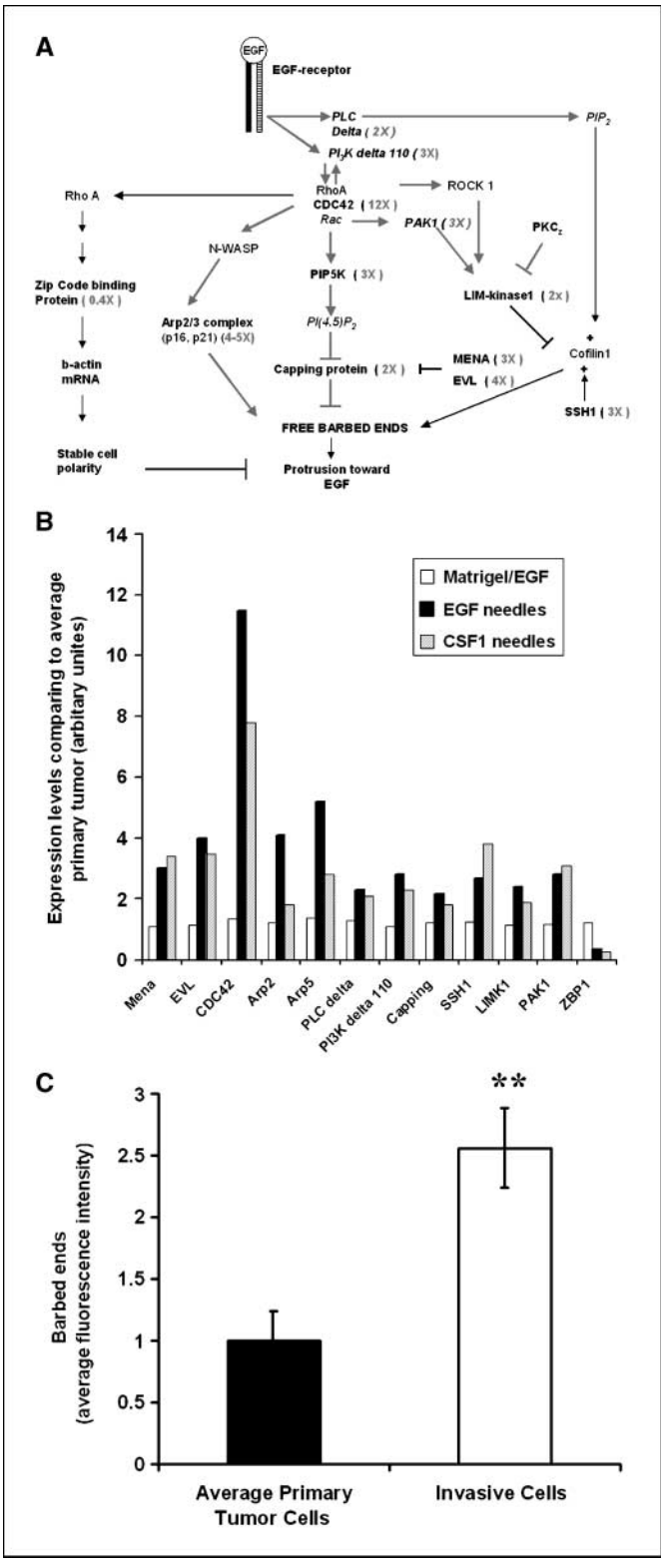

Figure 3. *A,* genes of the cell motility part of the invasion signature fall into coordinately regulated pathways leading to the initiation of protrusive force and chemotaxis. *nx,* fold changes in gene expression. *Right,* the cofilin pathway leading to the barbed end production in response to EGF. Genes for both inhibitory (PAK, LIMK 1) and stimulatory (SSH1) inputs to cofilin are more highly expressed in invasive cells. These regulate the location, timing, and sharpness of cofilin-dependent actin polymerization transient that is required for chemotaxis. *Middle,* capping protein pathway leading to barbed end capping. Genes for both inhibition (Mena, EVL, and PIP5K) and stimulation (capping protein) parts of the capping activity of this pathway are more highly expressed in invasive cells. To the left is the Arp2/3 complex pathway, which leads to dendritic nucleation in response to EGF. Genes coding for Arp2/3 complex subunits and upstream activators are more highly expressed in invasive cells. *Left,* the ZBP1 pathway, which regulates epithelial polarity by targeting key mRNAs that define the location of actin polymerization. ZBP1, a metastasis suppressor, is specifically down-regulated in the invasive cells of PyMT mammary tumors. *B,* validation of microarray results for selected genes by quantitative real-time PCR (QRT-PCR) shows that invasive tumor cells collected with both EGF and CSF1 show the same expression pattern. Expression analyses of invasive cells compared with the general population of cells in the tumor by QRT-PCR gives the same pattern for both ligands and is the same results obtained with cDNA microarrays. *C,* EGF-induced and cofilin pathway–dependent early transient of barbed ends is increased in invasive tumor cells from PyMT mammary tumors. The barbed end number was measured in the general population of tumor cells isolated from the primary tumor isolated by FACs sorting compared with invasive tumor cells isolated from the primary tumor using the *in vivo* invasion assay. *Columns,* quantization of the barbed end staining at 1 min after EGF stimulation. *Bars,* SE from at least 25 cells collected in three independent experiments. **, $P < 0.01$.

activity, which creates barbed ends that elongate to form newly polymerized actin filaments that stimulate the activity of the Arp2/3 complex (20). This synergistic amplification of the Arp2/3 complex activity has been proposed to explain the ability of cofilin to determine sites of protrusion and cell direction in uncaging experiments (22). Cofilin has also been found to amplify and stabilize N-WASP–generated invadopods, suggesting that the synergistic interaction between the cofilin and Arp2/3 complex pathways described above is at work during invasion (19, 22).

A gene in which expression is strongly down-regulated in invasive cells from the PyMT tumors is ZBP1. This is consistent with our previous study of MTLn3 cell line–derived tumors where ZBP1 was found to be down-regulated in invasive cells, consistent with its strong metastasis suppression activity (7). The invasion and metastasis suppression activity of ZBP1 seem to result from its ability to suppress the chemotaxis of cancer cells by maintaining them as polarized epithelial cells. ZBP1 may determine the sites in cells where the Arp2/3 complex, capping protein, and cofilin pathways converge to define the leading edge and, therefore, cell polarity by controlling the sites of targeting of β-actin and Arp 2/3 subunit mRNA, and the location of β-actin protein that is the common downstream effector of these pathways (23).

Cofilin pathway-associated changes in cell behavior and gene expression are conserved in both rat and mouse mammary tumors. It is of particular significance that the genes coding for both the stimulatory (*SSH1*) and inhibitory parts (*PAK1, LIMK 1*) of the cofilin pathway are up-regulated in invasive tumor cells of PyMT tumors (Fig. 3*A*; Table 1). This pattern of up-regulation of antagonistic effectors was seen before in the MTLn3 cell-derived rat mammary tumors, where both *cofilin 1* and *LIMK 1*, which are antagonistic to each other's effects on the output of the cofilin pathway, were up-regulated (7). However, the regulated genes are slightly different in these two types of invasive tumor cells. Invasive cells from MTLn3 tumors have EGF receptors (EGFR) and cofilin up-regulated on the stimulatory side and rho-associated coiled-coil containing protein kinase 1 and LIM kinase up-regulated on the inhibitory side, whereas invasive cells from PyMT tumors have phospholipase C (PLC) and SSH up-regulated on the stimulatory side and PAK1 and LIM kinase up-regulated on the inhibitory side.

The up-regulation of genes that both increase and decrease cofilin pathway activity in invasive tumor cells in response to EGF stimulation is critical in the mechanism of chemotaxis to EGF by tumor cells (9, 13). It is the local stimulation of cofilin activity by PLC and SSH and the simultaneous global inhibition of cofilin by LIM kinase that allows amplification and sensing of the EGF gradient during chemotaxis in tumor cells (13). The simultaneous local activation and global inhibition of the cofilin pathway generate a sharp transient of actin polymerization facing the EGF stimulus (13, 14). This is measured as a transient of free actin filament barbed ends, and this can be used as a reliable measure of the output of the cofilin pathway and is directly correlated with invasive and metastatic potential (9).

To determine if the antagonistic pattern of gene expression in the cofilin pathway seen in invasive cells from PyMT tumors results in the elevation of cofilin pathway activity as was seen in invasive cells from cell line–derived tumors, although slightly different patterns of genes were regulated, we measured the EGF-induced early barbed end transient in invasive tumor cells from PyMT primary tumors as described previously (9). The number of barbed ends in invasive tumor cells was compared with the number of barbed ends generated in response to EGF in the FACS sorted general population of tumor cells from the same primary tumors (9). The results show that the EGF-induced cofilin-dependent early transient of barbed ends is selectively increased in the invasive tumor cell population, indicating that the cofilin pathway regulating the early transient has increased activity (Fig. 3*C*). This is the same result that was seen in invasive tumor cells from MTLn3 tumors (9).

These results are remarkable because they illustrate that the same strategy for chemotaxis to EGF is employed by invasive tumor cells in tumors with different genetic origins and histologic phenotype, and that different genes in the same pathway can be altered to achieve the same phenotype. This result emphasizes that it is the activity of the pathway as a whole and not the change in expression of any one particular gene that determines the invasive and metastatic phenotype of the tumor. This has important implications for the future interpretation of expression profiling results. Furthermore, because certain pathways within the invasion signatures of both rat and mouse mammary tumors are conserved in their regulation, such pathways are prime candidates as targets for the treatment of tumor cell invasion and metastasis.

Acknowledgments

Received 10/6/2006; revised 2/19/2007; accepted 3/2/2007.

Grant support: NIH CA100324 and CA113395. We are grateful to members of the Center for Biophotonics and the Albert Einstein College of Medicine Microarray Facility for support and advice.

The costs of publication of this article were defrayed in part by the payment of page charges. This article must therefore be hereby marked *advertisement* in accordance with 18 U.S.C. Section 1734 solely to indicate this fact.

References

1. Wang W, Wyckoff JB, Frohlich VC, et al. Single cell behavior in metastatic primary mammary tumors correlated with gene expression patterns revealed by molecular profiling. Cancer Res 2002;62:6278–88.
2. Webster MA, Muller WJ. Mammary tumorigenesis and metastasis in transgenic mice. Semin Cancer Biol 1994;5:69–76.
3. Lin EY, Jones JG, Li P, et al. Progression to malignancy in the polyoma middle T oncoprotein mouse breast cancer model provides a reliable model for human diseases. Am J Pathol 2003;163:2113–26.
4. Kawamoto S, Niwa H, Tashiro F, et al. A novel reporter mouse strain that expresses enhanced green fluorescent protein upon Cre-mediated recombination. FEBS Lett 2000;470:263–8.
5. Wyckoff J, Wang W, Lin EY, et al. A paracrine loop between tumor cells and macrophages is required for tumor cell migration in mammary tumors. Cancer Res 2004;64:7022–9.
6. Wyckoff JB, Jones JG, Condeelis JS, Segall JE. A critical step in metastasis: *in vivo* analysis of intravasation at the primary tumor. Cancer Res 2000;60:2504–11.
7. Wang W, Goswami S, Lapidus K, et al. Identification and testing of a gene expression signature of invasive carcinoma cells within primary mammary tumors. Cancer Res 2004;64:8585–94.
8. Goswami S, Wang W, Wyckoff JB, Condeelis JS. Breast cancer cells isolated by chemotaxis from primary tumors show increased survival and resistance to chemotherapy. Cancer Res 2004;64:7664–7.
9. Wang W, Mouneimne G, Sidani M, et al. The activity status of cofilin is directly related to invasion, intravasation, and metastasis of mammary tumors. J Cell Biol 2006;173:395–404.
10. Sidani M, Wyckoff J, Xue C, Segall JE, Condeelis J. Probing the microenvironment of mammary tumors using multiphoton microscopy. J Mammary Gland Biol Neoplasia 2006;11:151–63.
11. Wyckoff JWY, Lin E, Li J, et al. Direct visualization of macrophage-assisted tumor cell intravasaton in mammary tumors. Cancer Res 2007;67:2649–56.
12. Quaranta V, Giannelli G. Cancer invasion: watch your neighbourhood! Tumori 2003;89:343–8.

13. Mouneimne G, DesMarais V, Sidani M, et al. Spatial and temporal control of cofilin activity is required for directional sensing during chemotaxis. Curr Biol 2006;16: 2193–205.
14. Mouneimne G, Soon L, DesMarais V, et al. Phospholipase C and cofilin are required for carcinoma cell directionality in response to EGF stimulation. J Cell Biol 2004;166:697–708.
15. Goswami S, Sahai E, Wyckoff JB, et al. Macrophages promote the invasion of breast carcinoma cells via a colony-stimulating factor-1/epidermal growth factor paracrine loop. Cancer Res 2005;65:5278–83.
16. Bear JE, Svitkina TM, Krause M, et al. Antagonism between Ena/VASP proteins and actin filament capping regulates fibroblast motility. Cell 2002;109:509–21.
17. Ho HY, Rohatgi R, Lebensohn AM, et al. Toca-1 mediates Cdc42-dependent actin nucleation by activating the N-WASP-WIP complex. Cell 2004; 118:203–16.
18. Mizutani K, Miki H, He H, Maruta H, Takenawa T. Essential role of neural Wiskott-Aldrich syndrome protein in podosome formation and degradation of extracellular matrix in src-transformed fibroblasts. Cancer Res 2002;62:669–74.
19. Yamaguchi H, Lorenz M, Kempiak S, et al. Molecular mechanisms of invadopodium formation: the role of the N-WASP-Arp2/3 complex pathway and cofilin. J Cell Biol 2005;168:441–52.
20. Ichetovkin I, Grant W, Condeelis J. Cofilin produces newly polymerized actin filaments that are preferred for dendritic nucleation by the Arp2/3 complex. Curr Biol 2002;12:79–84.
21. DesMarais V, Macaluso F, Condeelis J, Bailly M. Synergistic interaction between the Arp2/3 complex and cofilin drives stimulated lamellipod extension. J Cell Sci 2004;117:3499–510.
22. Ghosh M, Song X, Mouneimne G, Sidani M, Lawrence DS, Condeelis JS. Cofilin promotes actin polymerization and defines the direction of cell motility. Science 2004; 304:743–6.
23. Mingle LA, Okuhama NN, Shi J, Singer RH, Condeelis J, Liu G. Localization of all seven messenger RNAs for the actin-polymerization nucleator Arp2/3 complex in the protrusions of fibroblasts. J Cell Sci 2005;118:2425–33.